1521-009X/48/11/1239–1245$35.00
Drug Metabolism and Disposition

https://doi.org/10.1124/dmd.120.000194
Drug Metab Dispos 48:1239–1245, November 2020

Pharmacokinetics and Catabolism of [^{3}H]TAK-164, a Guanylyl Cyclase C Targeted Antibody-Drug Conjugate

Jayaprakasam Bolleddula,[1] Abhi Shah, Mohammad Shadid,[2] Afrand Kamali,[3] Michael D. Smith, and Swapan K. Chowdhury

Drug Metabolism and Pharmacokinetics Department (J.B., A.S., M.S., A.K., S.K.C.) and Oncology Drug Discovery Unit (M.D.S.), Millennium Pharmaceuticals, Inc., a wholly owned subsidiary of Takeda Pharmaceutical Company Limited, Cambridge, Massachusetts

Received July 22, 2020; accepted August 18, 2020

ABSTRACT

TAK-164 is an antibody-drug conjugate (ADC) comprising human anti–guanylyl cyclase C (GCC) monoclonal antibody conjugated to indolinobenzodiazepine DNA alkylator IGN-P1 through a cleavable alanine-alanine dipeptide linker. TAK-164 is currently being evaluated for the treatment of gastrointestinal cancers expressing GCC. The catabolism of TAK-164 was studied using ^{3}H-labeled ADC using GCC-expressing HEK-293 (GCC-HEK-293) cells, rat tritosomes, cathepsin B, and tumor-bearing mice. Time- and target-dependent uptake of [^{3}H]TAK-164 was observed in GCC-HEK-293 cells with approximately 12% of radioactivity associated with DNA after 24 hours of incubation. Rat liver tritosomes and cathepsin B yielded IGN-P1 aniline, sulfonated IGN-P1 (s-IGN-P1) aniline, and a lysine conjugate of IGN-P1 (IGN-P1-Lys) aniline as catabolites. In tumor-bearing mice, [^{3}H]TAK-164 exhibited a terminal half-life of approximately 41 and 51 hours in plasma and blood, respectively, with low plasma clearance (0.75 ml/h per kilogram). The extractable radioactivity in plasma and tumor samples revealed the presence of s-IGN-P1 aniline and IGN-P1 aniline as payload-related components. The use of a radiolabeled payload in the ADC in tumor uptake investigations provided direct and quantitative evidence for tumor uptake, DNA binding, and proof of mechanism of action of the payload.

SIGNIFICANCE STATEMENT

Since payload-related species are potent cytotoxins, a thorough characterization of released products of ADCs, metabolites, and their drug interaction potential is necessary prior to clinical investigations. This study characterized in vitro and in vivo DNA binding mechanisms and released products of TAK-164. The methodologies described here will be highly useful for characterization of payload-related products of ADCs in general.

Introduction

The achievement of balance between potency and safety for cancer drugs is still challenging. Recently, there has been a significant effort in optimizing the drug delivery strategies of cytotoxic molecules to minimize systemic toxicity while maintaining the desired efficacy (Lu and Qiao, 2018). Use of antibody-drug conjugates (ADCs) is one such strategy that has been gaining traction (Abdollahpour-alitappeh et al., 2019). The clinical proof of concept of ADCs as a modality for treating cancer has already been established through approval of eight ADCs thus far. These include brentuximab vedotin (Adcetris) for the treatment of CD30-positive cancers, such as Hodgkin lymphoma and systemic anaplastic large-cell lymphoma; ado-trastuzumab emtansine (Kadcyla) for the treatment of HER2-positive metastatic breast cancer; inotuzumab ozogamicin (Besponza) for the treatment of adults with relapsed or refractory B-cell precursor acute lymphoblastic leukemia; recently reintroduced gemtuzumab ozogamicin (Mylotarg) for newly diagnosed and relapsed or refractory CD33-positive acute myeloid leukemia (Coats et al., 2019); and more recently, Lumoxiti, Polivy, Enhertu, and Trodelvy for the treatment of adult patients with relapsed or refractory hairy cell leukemia, diffuse large B-cell lymphoma, unresectable or metastatic HER2-positive breast cancer, and metastatic triple-negative breast cancer, respectively (Cai and Kivel, 2019, https://www.adcreview.com/polatuzumab-vedotin-drug-description/).

An ADC consists of a recombinant monoclonal antibody linked to a highly potent cytotoxic small molecule through a linker via an amino group of lysine or thiol group of cysteines. ADCs act through binding to tumor-specific antigens expressed on the cancer cell membrane and deliver cytotoxic payloads via internalization and endosomal/lysosomal or pH-dependent degradation. The selective delivery of cytotoxic payloads improves the efficacy and safety profiles of ADCs by lowering systemic exposure. The cleavage mechanism and stability of ADCs depends on the type of linkers, i.e., cleavable or noncleavable. Cleavable linkers release free payload/catabolite(s), and noncleavable linkers release payload along with linker and an amino acid (cysteine or lysine) (Shadid et al., 2017). The free payload or catabolites released in the lysosomal compartment sometimes reach systemic circulation, and

This work was supported by Takeda Pharmaceutical Company Limited.
[1]Current affiliation: Agios Pharmaceuticals Inc., Cambridge, Massachusetts.
[2]Current affiliation: Sarepta Therapeutics, Cambridge, Massachusetts.
[3]Current affiliation: Kintai Therapeutics, Cambridge, Massachusetts.
All the authors are current or former employees of Takeda Pharmaceutical Company Limited and declare no competing interests.
https://doi.org/10.1124/dmd.120.000194.

ABBREVIATIONS: ADC, antibody-drug conjugate; CL, clearance; FA, formic acid; GCC, guanylyl cyclase C; HEK, human embryonic kidney; HER2, human epidermal growth factor receptor 2; HPLC, high-performance liquid chromatography; IGN, indolinobenzodiazepine; LSC, liquid scintillation counter; PBD, pyrrolobenzodiazepine dimer; PK, pharmacokinetics; s-IGN-P1, sulfonated IGN-P1; $t_{1/2}$, terminal elimination half-life; TRA, total radioactivity.

hence their identification and the determination of the concentration of free payload in plasma and tumor are necessary to understand toxicity, pharmacokinetics, and the PK-pharmacodynamics relationship (Shah et al., 2012; Diamantis and Banerji, 2016). Ultimately, the proper selection of antibody, linker, and payload will impact the ADC efficacy, safety, therapeutic index, exposure, and mechanism of catabolism. In addition, there should be mechanistic understanding of ADC disposition in early drug developmental stages to elucidate safety and efficacy.

Pyrrolobenzodiazepine dimers (PBDs) are a highly potent and novel class of payload that are being used in many ADCs in clinical development. PBDs are derived from conjugation of monomers to yield two imine functional groups that cross-link DNA through the N2 position of guanine (Gregson et al., 2019). Recently ImmunoGen developed new indolinobenzodiazepine dimers with monoimine functionality that covalently bind one strand of DNA to retain potency of di-imine without off-target toxicity of di-imine (Miller et al., 2016). TAK-164 (5F9 IGN-P1) is an ADC that consists of the human anti–guanylyl cyclase C (GCC) monoclonal antibody (IgG1) conjugated to indolinobenzodiazepine (IGN) dimer payload with monoamine through a cleavable alanine-alanine dipeptide linker (Abu-Yousif et al., 2017). GCC antigen is expressed in many gastrointestinal cancers, such as pancreatic, gastric, esophageal, and colorectal cancers. Although the GCC antigen is primarily expressed in the apical side in normal intestinal epithelial cells, access from the vascular compartment is restricted because of cell tight junctions. In cancer cells, apical localization of GCC antigens is disrupted, and hence GCC antigen became an attractive target for ADC-based drug delivery in gastrointestinal cancers (Park et al., 2002; Hyslop and Waldman, 2013; Almhanna et al., 2016). TAK-164 is being developed for the treatment of gastrointestinal cancers. The current article describes catabolism of [^{3}H]TAK-164 in rat tritosomes, human liver cathepsin B, GCC-expressing cells, and the pharmacokinetics and catabolism in tumor-bearing mice.

Materials and Methods

Test Articles and Reagents. Reference standards, IGN-P1 aniline, sulfonated IGN-P1 (s-IGN-P1) aniline, IGN-P1-Lys, [^{3}H]TAK-164, and chKTI-[^{3}H]IGN-P1 were provided by ImmunoGen. Rat liver tritosomes are lysosomes isolated from tyloxapol (surfactant)-treated rats and were purchased from Sekisui XenoTech, LLC. Human liver cathepsin B and other chemicals were obtained from Sigma-Aldrich Company LLC (St Louis, MO). SOLVABLE reagent and Ultima Gold scintillation cocktail were purchased from PerkinElmer (Waltham, MA). Gentra Puregene Cell and DNeasy Blood and Tissue kit for DNA isolation used for DNA isolation from cell and tissue, respectively, were purchased from Quiazen (Frederick, MA). Scintillation cocktail for online radioactivity detector was obtained from LabLogic System, Inc. (Tampa, FL).

Incubation of [^{3}H]TAK-164 with Target-Expressing Cells. GCC-expressing HEK-293 cells (0.6×10^6) were treated with 1 μg/ml of [^{3}H]TAK-164 or chKTI-[^{3}H]IGN-P1 in Dulbecco's modified Eagle's medium in a humidified incubator at 37°C. The concentration of ADC was selected to allow sufficient levels to elucidate the catabolism without causing cell death. Cells were harvested at 0, 4, and 24 hours and centrifuged (1000 rpm at 4°C) for 10 minutes to separate the cell pellet from the media. The cell pellet was washed with PBS, and 1.0 ml of acetone was added. The samples were stored at −80°C to allow for complete protein precipitation (30 minutes), and then the supernatant was separated by centrifugation. Similarly, medium was extracted with three volumes of acetone. The supernatant was separated from the media pellet. The acetone extracts from the cell and media pellets were dried separately under nitrogen and reconstituted with acetone:water (80:20, v:v), and the radioactivity was measured. The cell and media pellets were solubilized in SOLVABLE reagent overnight in a 50°C water bath and added to 50 μl of 100 mM disodium ethylenediaminetetraacetic acid and 100 μl of 30% H_2O_2. The samples were incubated for 1 hour at 50°C, 1 N HCl was added to each vial, and then the samples were left in the dark for 2 hours. The radioactivity was measured by adding 5 ml of Ultima Gold scintillation cocktail (PerkinElmer). Cell viability was measured at each time point, and total radioactivity was normalized to the number of live cells.

DNA Isolation from Cells. DNA from the cell pellet was isolated using Gentra Puregene Cell Kit according to the manufacturer's instructions. Briefly, the cells were washed, cell pellet was vortexed vigorously, and lysis buffer was added. The cells were vortexed for 10 seconds, and proteinase K solution was added to each tube. The contents were mixed thoroughly by inverting 25 times. Samples were incubated for 1 hour at 55°C and then cooled to 37°C. RNase A Solution (3 μl) was then added, and the samples were mixed, incubated for 5 minutes at 37°C, and then placed on ice for 3 minutes. Protein precipitation solution (200 μl) was added to each tube, and the samples were vortexed vigorously for 20 seconds and then placed on ice for 20 minutes. The tubes were then centrifuged for 10 minutes (4100 rpm at 4°C) to separate proteins. The supernatant was added to 600 μl of ice-cold isopropanol in a clean 1.5-ml microcentrifuge tube, mixed thoroughly, and centrifuged for 10 minutes. The supernatant was carefully discarded, and the DNA pellet was separated. The DNA pellet was dissolved in water, and total radioactivity was measured.

Incubation of [^{3}H]TAK-164 with Rat Liver Tritosomes and Human Cathepsin B. Rat liver tritosomes are lysosomes isolated from tyloxapol (surfactant)-treated rats. [^{3}H]TAK-164 (1 μM) was incubated with tritosomes derived from Sprague-Dawley rats (1 mg/ml) or human liver cathepsin B in a buffer containing 352 mM potassium phosphate monobasic, 48 mM sodium phosphate dibasic, and 4.0 mM EDTA. The pH was adjusted to 6.0 using 1 N HCl or 1 N potassium hydroxide. At 0, 24, and 48 hours, a 150-ml aliquot was separated, an equal amount of acetone was added, and the sample was placed on ice for 15 minutes to allow for protein precipitation. The samples were then centrifuged to separate the protein pellets. The supernatant from 24 hours of incubation was dried under nitrogen, and the residue was reconstituted in mobile phase A [0.1% formic acid (FA) in water] and mobile phase B (0.1% FA in acetonitrile), 80:20 (v:v), and then analyzed using high-performance liquid chromatography (HPLC) equipped with a β-particle emission radioactivity monitor.

Tumor-Bearing Mice. Immunodeficient nude female mice, NU-*Foxn1*^{nu} (Charles River Laboratories, Wilmington, MA), were inoculated with HEK-293

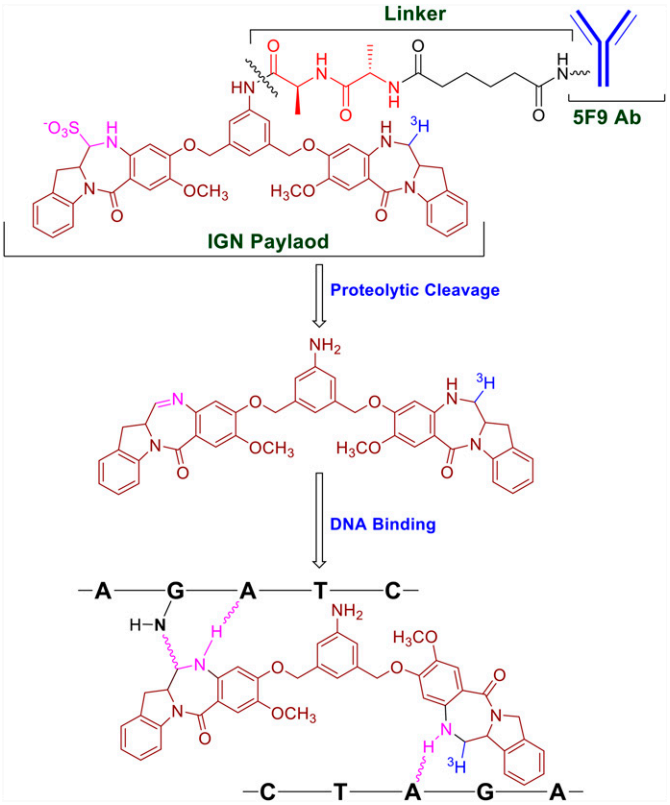

Fig. 1. Cleavage and DNA binding mechanism of [^{3}H]TAK-164. Ab, antibody..

TABLE 1

Percent total radioactivity measured after treatment of GCC-expressing HEK-293 cells with [^{3}H]TAK-164 and chKTI-[3H]IGN P1 (isotype control)

	Percent Total Radioactivity									
	Cell Extract		Media Extract		Media Pellet		Cell Pellet		DNA	
	0 h	24 h	0 h	24 h	0 h	24 h	0 h	24 h	0 h	24 h
chKTI-[^{3}H]IGN P1	0.25	0.28	4.41	2.78	89.20	90.65	6.14	6.30	0.33	1.57
[^{3}H]TAK-164	0.28	1.98	4.02	6.38	75.30	59.29	20.40	32.35	1.35	12.31

cells overexpressing GCC at Takeda, Cambridge, MA, and shipped to Covance (Greenfield, IN). The in-life portion of the study was conducted at Covance. After acclimatization, mice were divided into groups (n = 4 or 5) with unrestricted access to water and food (2920X; Teklad Global Diets). Animals were housed in a room with standard environmental conditions (temperature: 68–79°F; relative humidity: 30%–70%; 12-hour light/dark cycle). The dosing solution (1 mg/ml) was prepared in 20 mM histidine, 50 mM sodium chloride, 8.5% sucrose, and 50 μM sodium bisulfite (pH 6.2). [^{3}H]TAK-164 dosing (5 mg/kg; equivalent to 90 μg/kg of payload dose) was initiated when tumor volumes averaged approximately 250 mm^3 by intravenous infusion once at a dose volume of 5 ml/kg. The payload concentration (90 μg/kg) was calculated based on drug-to-antibody ratio (2.5) and the targeted dose (5 mg/kg). Blood, tumor, and liver tissues were collected at 0.25, 4, 48, 96, and 168 hours postdose. Blood was split into two aliquots. One aliquot was used for total radioactivity (TRA) analysis, the other aliquot was centrifuged, and plasma was separated. All tissues were immediately frozen in liquid nitrogen and stored at ≤ −60°C until they were processed for measurement of TRA or DNA isolation.

Total radioactivity in blood, plasma, and tissue homogenates was measured in duplicate using Ultima Gold XR scintillation cocktail on model 2900TR liquid scintillation counters (LSC; Packard Instrument Company) for at least 5 minutes or 100,000 counts. Scintillation counting data (counts per minute) were automatically corrected for counting efficiency using the external standardization technique and an instrument-stored quench curve generated from a series of sealed quenched standard. Plasma was mixed, and duplicate weighed aliquots were analyzed directly by LSC. For blood samples, a sufficient amount of commercial solubilizing agent was added to digest each sample. Samples were incubated for at least 1 hour at approximately 60°C, 0.1 M disodium EDTA was added to reduce foaming, and 30% hydrogen peroxide was added to remove color. The samples were allowed to sit at least overnight to allow any foaming to dissipate. Scintillation cocktail was added, and the samples were shaken and analyzed by LSC. Liver tissue samples were homogenized, combusted, and analyzed by LSC. Duplicate weighed aliquots of the tumor homogenate were digested in sodium hydroxide and analyzed directly by LSC.

Tumor DNA Isolation. Qiagen DNeasy Blood and Tissue kit was used for DNA isolation from tumor according to the manufacturer's directions. Briefly, tumor tissue was cut into small pieces and placed into tubes with ATL buffer, a tissue lysis buffer. After addition of proteinase K, samples were incubated overnight at 56°C. To the lysed tissue, buffer AL (lysis buffer)/ethanol (400 μl) was added and mixed thoroughly by vortex. The sample was then pipetted into the DNeasy MiniSpin column placed in a 2-ml collection tube and centrifuged at ≥6000g (8000 rpm) for 1 minute. The process repeated with wash buffers AW1 and AW2 [centrifuged at 20,000g (14,000 rpm) for 3 minutes], which were supplied by the vendor. Finally, DNA was eluted with 200 μl of AE buffer. DNA was stored at approximately −70°C until further analysis.

Plasma and Tumor Sample Processing. An aliquot of pooled mouse plasma samples was added to three volumes of acetone and vortex-mixed for 5 minutes. The samples were kept in the −80°C freezer for 30 minutes to ensure complete protein precipitation and centrifuged. The supernatants were transferred to a scintillation vial, and radioactivity was measured with an LSC (LS6500; Beckman Coulter, Inc.). Tissue homogenates (tumor and liver) were weighed, and an equal amount of acetone was added. The mixture was mixed thoroughly (vortex) and sonicated for 5 minutes (twice) with minimal shaking in between; samples were placed in the freezer at −80°C for 30 minutes for precipitation of proteins. The mixture was centrifuged, and TRA of the supernatant was counted with LSC. For metabolite/catabolite profiling, the supernatants were transferred to glass tubes, and the solvent was evaporated under vacuum (SPD1010 Integrated

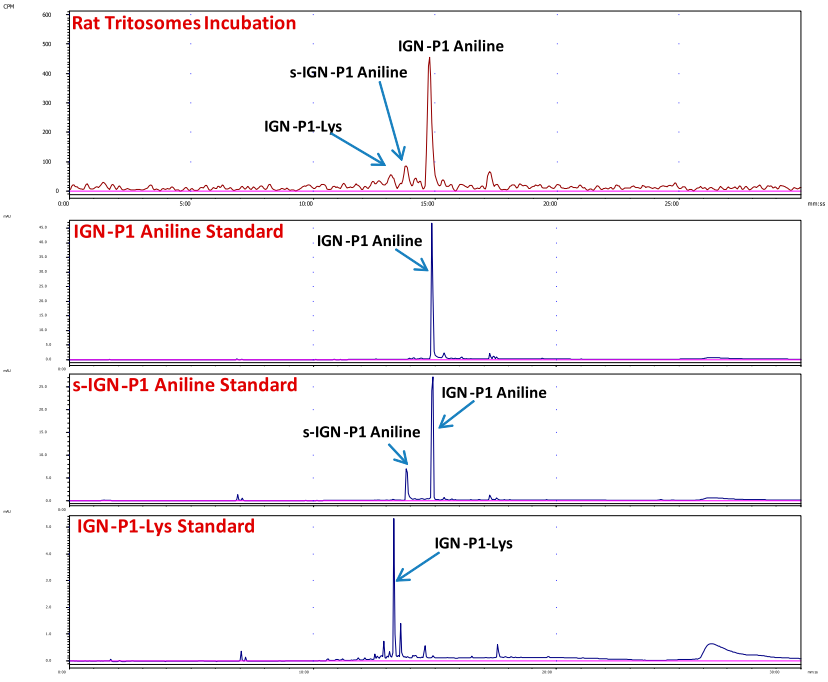

Fig. 2. Representative radiochromatogram of catabolites of [^{3}H] TAK-164 after incubation in rat tritosomes over 24 hours.

TABLE 2

Pharmacokinetic parameters of total radioactivity ([^{3}H]TAK-164 equivalents) after a single intravenous administration of 5 mg/kg [^{3}H]TAK-164 to mice

Tumor and liver tissue parameters were calculated using extravascular dosing type. Plasma and blood parameters were calculated using intravenous dosing type.

Matrix	Dose	C_{max}	AUC_{last}	AUC_{∞}	AUC_{∞} %Extrapolated	CL	$t_{1/2}$
	mg/kg	*μg-eq/ml or g*	*h*μg-eq/ml or g*	*h*μg-eq/ml or g*	*%*	*ml/h per kilogram*	*h*
Blood	5	72.4	3490	3840	9.2	1.30	50.5
Plasma	5	116	6370	6720	5.1	0.745	41.2
Liver	5	20.2	1330	1858	28	NC	NC
Tumor	5	32.9	3630	5520	34	NC	NC
Tumor DNA	5	0.680	70.8	90.9	22	NC	NC

AUC_{last}, area under concentration-time curve from 0 to time of the last quantifiable concentration; NC, not calculated. AUC_{∞} % Extrap (% extrapolated), % area under concentration time curve from 0-infinity.

SpeedVac; Thermo Fisher Scientific, Waltham, MA). The dried samples were then reconstituted in 200 μl of solvent (80% water and 20% acetone) for analysis.

Pharmacokinetic Calculations. Total radioactivity was measured by LSC and expressed in microgram-equivalents/gram (μg-eq/g). Pharmacokinetic analysis of plasma concentration data was performed with Phoenix WinNonlin, version 6.3 (Pharsight Corp, Mountain View, CA). PK parameters, including the observed C_{max}, time to maximum concentration, area under the concentration-time curve (AUC) from 0 to time of the last quantifiable concentration, extrapolated AUC from time 0 to infinity, clearance (CL), volume of distribution at steady state, and terminal half-life ($t_{1/2}$), were estimated using noncompartmental models. Tumor tissue samples were derived using extravascular dosing type based on the gradual increase in tumor concentrations from 0 to 96 hours, followed by a decline in concentrations. The AUC was calculated using the linear trapezoidal rule. Graphs included in this report were plotted in Phoenix WinNonlin (Pharsight Corp).

Liquid Chromatography and Radioactivity Detection. Liquid chromatography was performed using an Agilent 1290 HPLC system with a binary pump, autosampler, and diode array detector coupled to a Kinetex C18 column (2.6 μM, C18, 4.6 × 150 mm, 100 A) (Phenomenex, Inc., Torrance, CA) at 40°C column temperature. Solvent A was 0.1% FA in water, and solvent B was 0.1% FA in acetonitrile. The gradient started with 5% B (0–3 minute), followed by 95% B (3–24 minute) with a hold up to 26 minutes at 95% B and back to starting conditions (5% B) from 26 to 30 minutes. The reconstituted samples were analyzed by HPLC with online radioactive detector (β-particle emission radioactivity monitor, model), or eluent was collected into Isoplate 96-well plates (PerkinElmer Life Sciences, Inc., Waltham, MA). The solvent in the plates was evaporated and mixed with Microscint PS scintillation cocktail (50 μl) (PerkinElmer Life Sciences, Inc). The radioactivity was counted using MicroBeta Trilux (PerkinElmer Life Sciences, Inc). Radiochromatograms were constructed using Laura software (LabLogic Systems Limited, Brandon, FL).

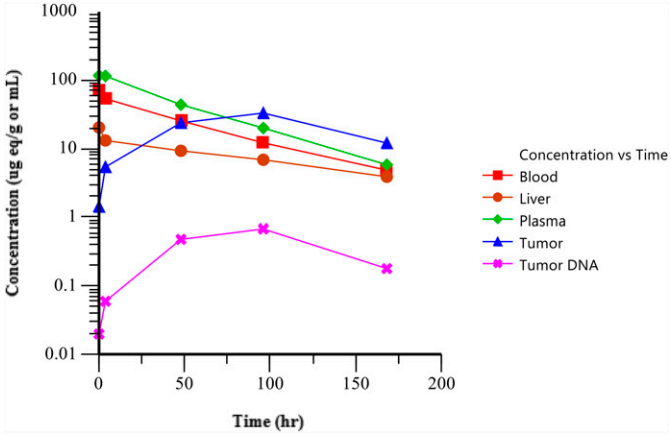

Fig. 3. Mean concentration-time curves for total radioactivity measured across various matrices after a single intravenous administration of TAK-164 to xenograft mice.

Structures were identified by comparison of retention times with authentic standards and mass spectra. The retention times and shape of the radioactive peaks varied because of matrix effect. However, authentic standards were analyzed in the same run and/or mass spectra were collected to unambiguously assign the structures. The liquid chromatography-mass spectrometry analysis was performed with AB Sciex 6500 triple quadrupole mass spectrometry (AB SCIEX, Framingham, MA) using positive ionization mode with the following conditions: collision energy = 37 v, curtain gas = 25 (arbitrary units), declustering potential = 71, source temperature = 600°C, and multiple reaction monitoring transitions are 708→247 (IGN-P1 aniline) and 790→708 (sulfonyl IGN-P1 aniline) with HPLC conditions described above.

Results

TAK-164 is an ADC with fully humanized anti-GCC monoclonal antibody connected to indolinobenzodiazepine via cleavable ala-ala dipeptide linker (Abu-Yousif et al., 2017). In preclinical studies, TAK-164 exhibited a dose- and time-dependent increase in DNA damage and durable antitumor activity in multiple GCC-positive patient-derived xenografts after a single intravenous administration. Further imaging studies with tumor-bearing mice demonstrated that TAK-164 preferentially accumulates in GCC-positive tumors (Abu-Yousif et al., 2017). Since ADCs contain highly potent cytotoxic payloads, understanding of metabolites and catabolites derived from these small molecules is important in part because the catabolites may possess pharmacological, toxicological, and DDI potential.

The catabolism of TAK-164 was studied in vitro and in vivo using rat tritosomes, human liver cathepsin B, and GCC-expressing HEK-293 cells and in xenograft mice bearing GCC-HEK-293 subcutaneous tumors. Because of the ease of synthesis and to achieve high specific activity (2.11 Ci/mmol), TAK-164 was labeled with tritium (^{3}H) at an α-proton to the secondary nitrogen of tetrahydrodiazepinone (Fig. 1). The drug-to-antibody ratio in [^{3}H]TAK-164 ranged from 2.2 to 2.5. TAK-164 was designed with a cleavable linker to release sulfonated IGN-P1 aniline followed by desulfonation to form an active imine, which binds to DNA through nucleophilic addition (Fig. 1). chKTI-[^{3}H]IGN-P1, which was used as a negative control, is an ADC with the same payload and linker, but the antibody has no affinity for any mouse or human GCC antigen. Both [^{3}H]TAK-164 or chKTI-[^{3}H]IGN-P were incubated with GCC-expressing HEK-293 cells under similar conditions. After incubation, the cells were separated from media at 0, 4, and 24 hours. The media and cells were extracted with acetone, and extracts were separated to yield media extract, media pellet, cell extracts, and cell pellet, respectively. The majority of the radioactivity was recovered from the media and cell pellets. The radioactivity recovered in the media pellet resulted from the precipitation of intact ADC. The radioactivity in the cell pellet could be from intact ADC, free payload, or payload attached to

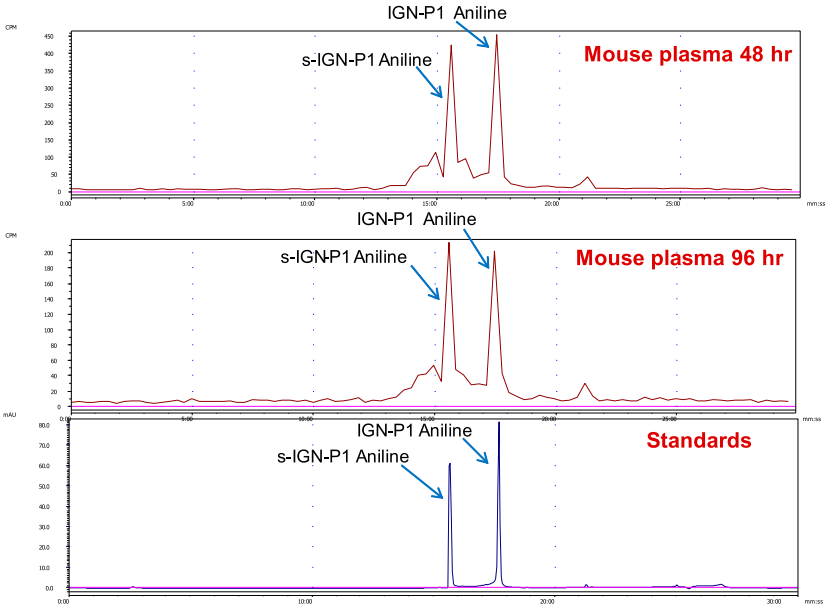

Fig. 4. Radiochromatograms of pooled plasma extracts at 48 hours (top panel) and 96 hours (middle panel) after intravenous administration of [^{3}H]TAK-164. The bottom panel shows the UV signal for sulfonyl IGN-P1 aniline reference standard at λ = 320 nm.

DNA. After treatment of cells with [^{3}H]TAK-164 and incubation for 24 hours, a time-dependent increase (~20%–32%) in cell pellet radioactivity and a time-dependent decrease in media pellet (~75%–59%) radioactivity revealed an uptake of ADC into cells that increased over time. Cell and media extract yielded <2% and <7%, respectively, of total radioactivity. In media extracts, even at time zero, approximately 4% of the total radioactivity was observed, suggesting that some residual ADC is present (Table 1). The profiling of these extracts did not yield any payload-related catabolites in media, suggesting very low levels of free payload–related material in the cell and media extracts. In incubation with chKTI-[^{3}H]IGN-P1 (isotype control), approximately 91% of the radioactivity was observed in media pellet, and cell extracts had negligible amounts of radioactivity. Media extract (3%–4%) and cell pellet (~6%) treated with isotype control (chKTI-[^{3}H]IGN-P1) had some radioactivity, but there was no change observed over time, suggesting this could be due to nonspecific binding of radioactivity to cells. Approximately 12% of radioactivity (approximately 38% of the total radioactivity observed in the cell pellet) was associated with DNA in cells treated with [^{3}H]TAK-164, whereas <2% radioactivity was associated with DNA in cells treated with chKTI-[^{3}H]IGN-P1 (isotype control) after 24 hours of incubation, suggesting target-dependent uptake of TAK-164.

Incubation of [^{3}H]TAK-164 with rat tritosomes yielded one major and two minor catabolites in acetone extract. The major catabolite was identified as IGN-P1 aniline, and the minor catabolites were determined to be sulfonated IGN-P1 aniline and IGN-P1-Lys. This was confirmed by comparison of retention times with authentic standards. Similarly, incubation of [H]TAK-164 with cathepsin B yielded two catabolites,

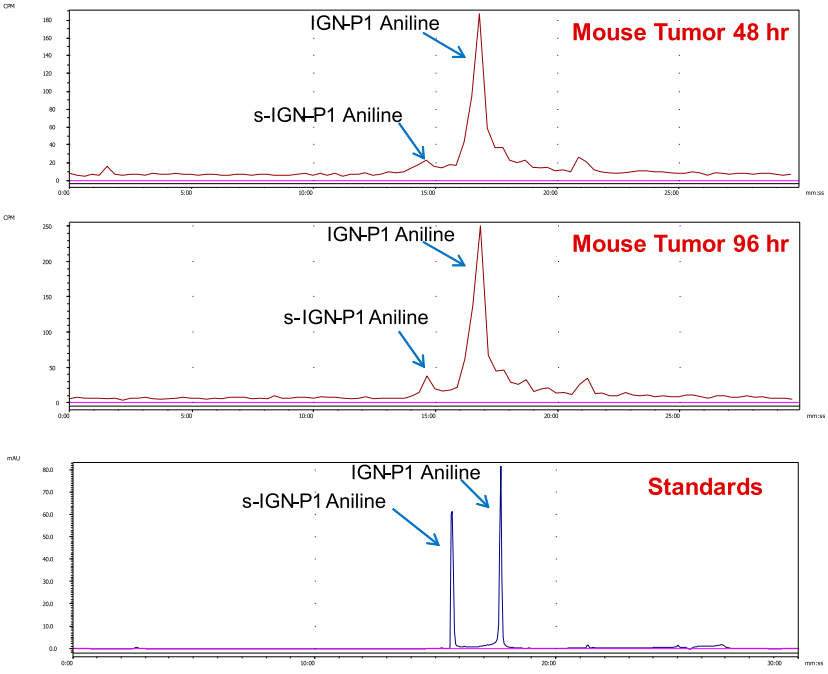

Fig. 5. Radiochromatograms of pooled tumor extracts at 48 hours (top panel) and 96 hours (middle panel) after intravenous infusion of [^{3}H]TAK-164. Bottom panel shows the UV signal for sulfonyl IGN-P1 aniline reference standard at λ = 320 nm.

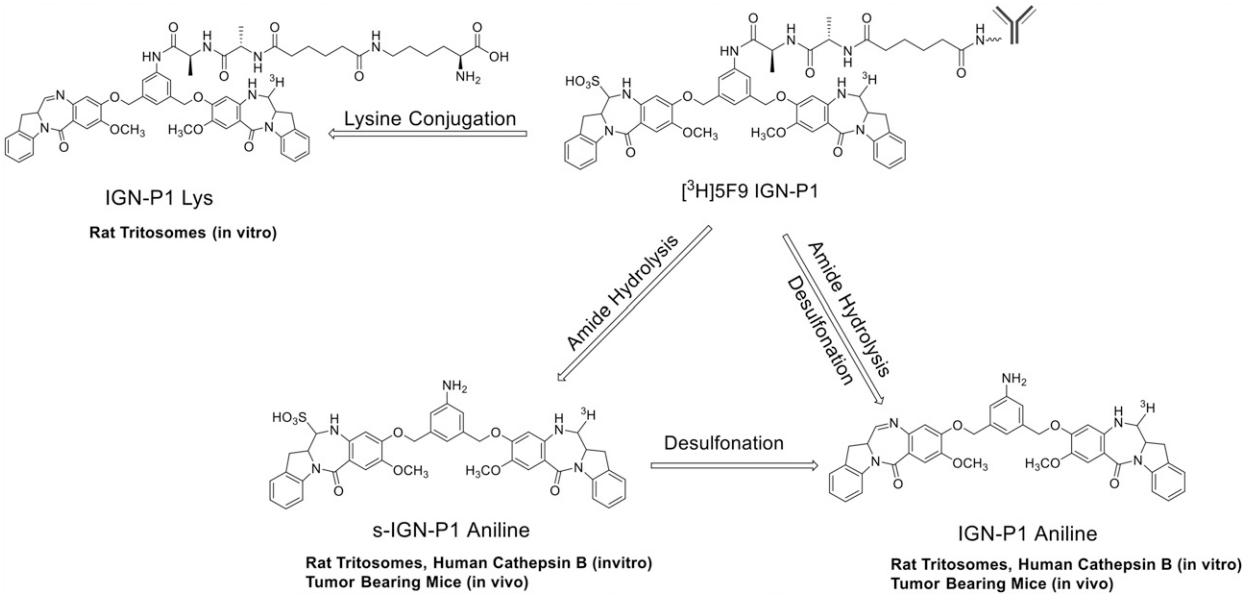

Fig. 6. Proposed biotransformation pathways of [^{3}H]TAK-164.

which were identified as IGN-P1 aniline and sulfonyl IGN-P1 aniline (Fig. 2).

In the in vivo experiment, 5 mg/kg [^{3}H]TAK-164 was administered to tumor-bearing mice inoculated with HEK-293 cells overexpressing GCC via intravenous infusion, and samples including blood, liver, and tumor specimen were collected at 0.25, 4, 48, and 168 hours. TRA was measured in blood and plasma directly. Tissue samples were homogenized, and TRA was measured. The C_{max} values in blood, plasma, liver, and tumor were 72, 116, 20, and 33 μg-eq/ml, respectively (Table 2). The TRA exhibited $t_{1/2}$ of approximately 41 and 51 hours in plasma and blood, respectively (Table 2). TAK-164 exhibited a low systemic plasma CL of 0.75 ml/h per kilogram. Plasma area under the concentration-time curve from time 0 to infinity (AUC_∞) (6720 hour*μg-eq/ml) was approximately 1.8 (3840 hour*μg-eq/ml), 3.6 (1858 hour*μg-eq/ml), and 1.2 (5520 hour*μg-eq/ml) greater than the blood, liver, and tumor, respectively. To obtain area under the curve from time 0-∝ (AUC_∞) in tumors, the area under the curve from time 0-t (AUC_t) was extrapolated to >30% (Table 2). A time-dependent increase of radioactivity in tumor DNA was observed (Fig. 3). Approximately 2% of the total radioactivity entering the tumor tissue was bound to DNA.

Metabolite/catabolite profiling of plasma revealed two major circulating catabolites (Fig. 4). The structures were identified as sulfonated IGN-P1 aniline and the desulfonated derivative, IGN-P1 aniline, by comparing the retention time with reference standards by UV spectrometry (λ = 320 nm) and/or liquid chromatography-mass spectrometry analysis. In tumor, the major radioactivity related peak corresponded to IGN-P1 aniline, whereas sulfonyl IGN-P1 aniline was a minor component (Fig. 5).

Discussion

Antigen expression and resynthesis, linker cleavage, payload permeability, and cell retention are major factors for driving efficacy of an ADC (Zhang et al., 2016). It is very important to get a mechanistic understanding of payload release and its concentration in tumor cells to establish the PK-pharmacodynamics relationship early in preclinical stages. Because of the lack of well established methods and extremely low levels of payloads, it has been challenging to identify the released products from ADCs. Target-expressing cancer cells have been used to study the catabolism of antibody-drug conjugates. A good in vitro–in vivo correlation was observed in catabolism of trastuzumab conjugates using an HER2$^+$-positive xenograft model (Erickson et al., 2012). The cleavage products of TAK-164 have been identified in vitro using cathepsin B enzyme and rat tritosomes, and DNA binding potential was studied using GCC-expressing HEK-293 cells. Rat liver tritosomes are highly purified hepatic lysosomes that contain a number of hydrolytic enzymes. Since not many in vitro assay systems are available to determine the catabolic fate of ADCs, rat tritosomes were used as an exploratory enzyme system to study the catabolism of TAK-164. This system provided consistent results with other in vitro systems to study catabolism of TAK-164. In both cathepsin B and rat liver tritosomal incubations, TAK-164 yielded cleavage products sulfonyl IGN-P1 aniline and IGN-P1 aniline, as expected (Fig. 6). In target-expressing cells, time-dependent uptake of TAK-164 into cells and DNA binding demonstrated efficient binding to antigen-expressing cells in vitro followed by catabolism inside the cell to yield free payload.

After a single intravenous administration of [^{3}H]TAK-164 GCC-positive xenografts, the total radioactivity-related [^{3}H]TAK-164 was measured in blood, plasma, liver, tumors, and tumor DNA. The pharmacokinetics of TAK-164–related total radioactivity displayed low plasma clearance (Table 2). Plasma had the highest concentration of total radioactivity compared with liver and tumor. TAK-164 partitioned into blood with a blood-to-plasma ratio of approximately 0.5. Detection of radioactivity at early time points in tumor and tumor DNA suggests a faster reach of TAK-164 to the site of action, with time to maximum concentration of approximately 48 hours. As shown in Table 2, the measured tumor and plasma exposures of total radioactivity were higher in plasma than tumors. The plasma AUC_∞ of [^{3}H]TAK-164 after intravenous administration (equivalent to 90 μg/kg of payload dose) to tumor-bearing mice was approximately 1.8-, 3.6-, 1.2-, and 74-fold greater than the blood, liver, tumor, and tumor DNA AUC_∞, respectively.

Since the samples were collected at limited time points, there is a possibility that C_{max} and $t_{1/2}$ might have been underestimated. In a previous study with nonradiolabeled TAK-164, a dose- and time-dependent increase in DNA damage as measured by the

pharmacodynamic marker pH2A.X in GCC-positive tumor-bearing xenografts was observed (Abu-Yousif et al., 2017). Furthermore, the use of preclinical imaging demonstrated that TAK-164 preferentially accumulates in GCC-positive tumors. Extraction of liver homogenates with acetone did not yield any catabolites; however, in tumor, IGN-P1 aniline was observed as a major catabolite. This finding suggests that the catabolites were released after tumor uptake of TAK-164, most likely in the lysosomes.

In previous studies, the ability of tumor DNA alkylation was investigated using ADCs with PBDs (Ma et al., 2016, 2020). The results from the current study provided detailed understanding of the nature of the catabolites of TAK-164 (with indolinobenzodiazepine payload) in the tumors and their DNA binding/alkylation properties. The radioactivity associated with tumor DNA was estimated as 2% of the total tumor radioactivity. The extent of DNA binding can be varied based on the type of payload and rate of its release. Two catabolites, s-IGN-P1 aniline and IGN-P1 aniline, were the major payload-related catabolites observed from in vitro studies. The uptake of [^{3}H]TAK-164 was target-dependent since no uptake was observed with chKTI-(^{3}H)IGN-P1, an isotype antibody with no affinity for GCC receptors. Similar results were observed in tumor-bearing mouse–derived GCC-expressing cell lines. Sulfonyl IGN-P1 aniline and IGN-P1 aniline are the major circulating catabolites in plasma, whereas IGN-P1 is the major catabolite in tumors. The radioactivity associated with DNA both in vitro and in vivo substantiated the mechanism of action of indolinobenzodiazepine as a DNA alkylator. This study underscores the importance of the use of a radiolabeled payload in the ADC in tumor uptake investigations, which provide direct and quantitative evidence for tumor uptake, DNA binding, and proof of mechanism of action of the payload and help to elucidate catabolism of an ADC.

Acknowledgments

The authors thank ImmunoGen, Inc., for providing tritium-labeled TK-164, tritium-labeled chKTI-IGN-P1, and reference standards of metabolites.

Authorship Contributions

Participated in research design: Bolleddula, Shah, Shadid, Kamali, Smith, Chowdhury.

Conducted experiments: Shah, Shadid, Kamali.

Performed data analysis: Bolleddula, Shah, Shadid, Kamali.

Wrote or contributed to the writing of the manuscript: Bolleddula, Shah, Chowdhury.

References

Abdollahpour-Alitappeh M, Lotfinia M, Gharibi T, Mardaneh J, Farhadihosseinabadi B, Larki P, Faghfourian B, Sepehr KS, Abbaszadeh-Goudarzi K, Abbaszadeh-Goudarzi G, et al. (2019) Antibody-drug conjugates (ADCs) for cancer therapy: strategies, challenges, and successes. *J Cell Physiol* **234**:5628–5642.

Abu-Yousif AO, Bannerman BM, Cvet D, Gallery M, Ganno ML, Smith MD, Lai KC, Keating TA, Bolleddula J, Stringer B, et al. (2017) TAK-164, a GCC-targeted antibody drug conjugate (ADC) for the treatment of colorectal cancers and other GI malignancies. In *Proceedings of the AACR-NCI-EORTC International Conference: Molecular Targets and Cancer Therapeutics: Discovery, biology, and clinical applications*; 2017 October 26–30, Philadelphia, PA.

Almhanna K, Kalebic T, Cruz C, Faris JE, Ryan DP, Jung J, Wyant T, Fasanmade AA, Messersmith W, and Rodon J (2016) Phase I study of the investigational anti-guanylyl cyclase antibody-drug conjugate TAK-264 (MLN0264) in adult patients with advanced gastrointestinal malignancies. *Clin Cancer Res* **22**:5049–5057.

Cai HH and Kivel N (2019) Therapeutic monoclonal antibodies approved by food and drug administration in 2018. *Clin Res Immunol* **2**:1–3.

Coats S, Williams M, Kebble B, Dixit R, Tseng L, Yao NS, Tice DA, and Soria JC (2019) Antibody-drug conjugates: future directions in clinical and translational strategies to improve the therapeutic index. *Clin Cancer Res* **25**:5441–5448.

Diamantis N and Banerji U (2016) Antibody-drug conjugates--an emerging class of cancer treatment. *Br J Cancer* **114**:362–367.

Erickson HK, Lewis Phillips GD, Leipold DD, Provenzano CA, Mai E, Johnson HA, Gunter B, Audette CA, Gupta M, Pinkas J, et al. (2012) The effect of different linkers on target cell catabolism and pharmacokinetics/pharmacodynamics of trastuzumab maytansinoid conjugates. *Mol Cancer Ther* **11**:1133–1142.

Gregson SJ, Tiberghien AC, Masterson LA, and Howard PW (2019) Pyrrolobenzodiazepine dimers as antibody–drug conjugate (adc) payloads, in *Cytotoxic Payloads for Antibody-Drug Conjugates* (Thurston DE and Jackson PJM 296–331, The Royal Society of Chemistry, Cambridge, UK.

Hyslop T and Waldman SA (2013) Guanylyl cyclase C as a biomarker in colorectal cancer. *Biomarkers Med* **7**:159–167.

Lu ZR and Qiao P (2018) Drug delivery in cancer therapy, quo vadis? *Mol Pharm* **15**:3603–3616.

Ma Y, Chen B, and Zhang D (2020) Quantitation of DNA by nuclease P1 digestion and UPLC-MS/MS to assess binding efficiency of pyrrolobenzodiazepine. *J Pharm Anal* **10**:247–252.

Ma Y, Khojasteh SC, Hop CECA, Erickson HK, Polson A, Pillow TH, Yu SF, Wang H, Dragovich PS, and Zhang D (2016) Antibody drug conjugates differentiate uptake and DNA alkylation of pyrrolobenzodiazepines in tumors from organs of xenograft mice. *Drug Metab Dispos* **44**:1958–1962.

Miller ML, Fishkin NE, Li W, Whiteman KR, Kovtun Y, Reid EE, Archer KE, Maloney EK, Audette CA, Mayo MF, et al. (2016) A new class of antibody-drug conjugates with potent DNA alkylating activity. *Mol Cancer Ther* **15**:1870–1878.

Park J, Schulz S, Haaf J, Kairys JC, and Waldman SA (2002) Ectopic expression of guanylyl cyclase C in adenocarcinomas of the esophagus and stomach. *Cancer Epidemiol Biomarkers Prev* **11**:739–744.

Shadid M, Bowlin S, and Bolleddula J (2017) Catabolism of antibody drug conjugates and characterization methods. *Bioorg Med Chem* **25**:2933–2945.

Shah DK, Haddish-Berhane N, and Betts A (2012) Bench to bedside translation of antibody drug conjugates using a multiscale mechanistic PK/PD model: a case study with brentuximab-vedotin. *J Pharmacokinet Pharmacodyn* **39**:643–659.

Zhang D, Yu SF, Ma Y, Xu K, Dragovich PS, Pillow TH, Liu L, Del Rosario G, He J, Pei Z, et al. (2016) Chemical structure and concentration of intratumor catabolites determine efficacy of antibody drug conjugates. *Drug Metab Dispos* **44**:1517–1523.

Address correspondence to: Jayaprakasam Bolleddula, Agios Pharmaceuticals, Inc., 88 Sidney St, Cambridge, MA 02139. E-mail: Jayaprakasam.bolleddula@agios.com